

Article

Synthesis and Structure of a New Iodate $\text{Cs}_5[\text{Sc}_2(\text{IO}_3)_9](\text{IO}_3)_2$ with a Complex Framework Based on the Condensation of $[\text{Sc}(\text{IO}_3)_6]$ Building Blocks

Olga V. Reutova ¹, Elena L. Belokoneva ^{1,*}, Anatoly S. Volkov ² and Olga V. Dimitrova ¹

¹ Department of Crystallography and Crystal Chemistry, Geological Faculty, Lomonosov Moscow State University, Moscow 119991, Russia; reutova.olia@yandex.ru (O.V.R.); dimitrova@list.ru (O.V.D.)

² Skolkovo Institute of Science and Technology, Moscow 121205, Russia; toljha@yandex.ru

* Correspondence: elbel@geol.msu.ru; Tel.: +7-495-939-4926

Abstract: Transparent single crystals of a new iodate $\text{Cs}_5[\text{Sc}_2(\text{IO}_3)_9](\text{IO}_3)_2$ were synthesized under mild hydrothermal conditions. X-ray diffraction of single crystal was used to determine the large crystal structure with 52 independent atoms, sp. gr. $P2_1/c$. The building blocks $[\text{Sc}(\text{IO}_3)_6]^{3-}$ of Sc octahedra and six (IO_3) groups are condensed into a framework; the structure contains additional isolated (IO_3) groups. Large Cs cations occupy holes and form an intercrossing framework. Similar building blocks $[\text{M}(\text{IO}_3)_6]$ are known for many iodates; however, most are isolated. Their topology and symmetry differ and determine the properties of the compounds.

Keywords: iodate; hydrothermal synthesis; single crystal structure; building block; complex framework



Citation: Reutova, O.V.; Belokoneva, E.L.; Volkov, A.S.; Dimitrova, O.V. Synthesis and Structure of a New Iodate $\text{Cs}_5[\text{Sc}_2(\text{IO}_3)_9](\text{IO}_3)_2$ with a Complex Framework Based on the Condensation of $[\text{Sc}(\text{IO}_3)_6]$ Building Blocks. *Symmetry* **2023**, *15*, 1777. <https://doi.org/10.3390/sym15091777>

Academic Editor: György Keglevich

Received: 11 August 2023

Revised: 12 September 2023

Accepted: 14 September 2023

Published: 17 September 2023



Copyright: © 2023 by the authors. Licensee MDPI, Basel, Switzerland. This article is an open access article distributed under the terms and conditions of the Creative Commons Attribution (CC BY) license (<https://creativecommons.org/licenses/by/4.0/>).

1. Introduction

Iodates are a class of inorganic compounds possessing I^{5+} ions in umbrella-like coordination in the form of $(\text{IO}_3)^-$ anionic groups. Due to the polar distribution of the electron density around the I^{5+} ions, many iodates with non-centrosymmetric structures are characterized by optical nonlinearity (e.g., well-known $\alpha\text{-LiIO}_3$ [1], $\alpha\text{-In}(\text{IO}_3)_3$ [2], $\text{BiO}(\text{IO}_3)$ [3], and others [4,5]). In the last decade, iodates have attracted attention as potential materials with not only optical nonlinearity, but also many other attractive characteristics, such as photoluminescence or magnetic properties. On the other hand, the compounds exhibit a wide variety of structures, which led to interest in structural and crystal chemical studies. Typically, (IO_3) groups have isolated positions; however, condensed iodate anions are also described, for example, in $\text{HBa}_{2.5}(\text{IO}_3)_6(\text{I}_2\text{O}_5)$ and $\text{HBa}(\text{IO}_3)(\text{I}_4\text{O}_{11})$ [6], or recently obtained $\text{K}_2\text{Na}(\text{IO}_3)_2(\text{I}_3\text{O}_8)$ [7].

One of the most important goals of material research is the directed synthesis of the desired crystals (the so-called tailoring design) or knowledge of the conditions for their production. Therefore, all new data on the correlation of synthesis and the resulting phases are important for further development.

Let us concentrate on iodate compounds, which have some structural features. There are many metal iodates containing the building blocks of a (MO_6) octahedron linked to six (IO_3) groups at the oxygen vertices. Isolated $[\text{M}(\text{IO}_3)_6]$ blocks of various symmetry are described for a series of compounds with tetravalent ($\text{M}^{\text{IV}} = \text{Ti, Ge, Sn, Pt}$) or trivalent ($\text{M}^{\text{III}} = \text{In, Sc, Fe, Ga}$) cations. Thus, in the group of structures of the general formula $\text{A}_2\text{M}(\text{IO}_3)_6$ ($\text{A} = \text{Li, Na, K, Rb, Cs, Tl, Ag, H}_3\text{O}$ and $\text{M} = \text{Ti, Ge, Sn, Pt}$) [8–14], most compounds are trigonal and possess a centrosymmetric $R\bar{3}$ space group. However, structures with small Li^+ and Na^+ cations have a polar space group $P6_3$ and exhibit nonlinear optical properties as well as $\text{BaGe}(\text{IO}_3)_6 \cdot \text{H}_2\text{O}$ [13], possessing noncentrosymmetric sp.gr. $R3$. Compounds $\text{SrTi}(\text{IO}_3)_6 \cdot 2\text{H}_2\text{O}$, $\text{SrSn}(\text{IO}_3)_6$ [14], $\text{BaTi}(\text{IO}_3)_6$ [15], and $\text{Ba}_3\text{Ga}_2(\text{IO}_3)_{12}$ [16] also consist of isolated $[\text{M}(\text{IO}_3)_6]$ blocks and have similar structures with trigonal sp.gr. $R\bar{3}$.

Recently investigated iodates with similar blocks, namely $\text{Rb}_3\text{Sc}(\text{IO}_3)_6$ (sp.gr. *Pc*) [17], $\text{K}_3\text{Sc}(\text{IO}_3)_6$ (sp.gr. *Fdd2*) [18], and $\alpha\text{-K}_3\text{In}(\text{IO}_3)_6$ (sp.gr. *Fdd2*) [19], form a family of nonlinear optical compounds $\text{A}_3\text{M}(\text{IO}_3)_6$ ($\text{A} = \text{K}, \text{Rb}$; $\text{M} = \text{Sc}, \text{In}$); iodates with analog formulas ($\beta\text{-K}_3\text{In}(\text{IO}_3)_6$ [19], $\text{Rb}_3\text{In}(\text{IO}_3)_6$ [20] and $\text{Na}_3\text{Fe}(\text{IO}_3)_6$ [21]) possess polar *P*-1 space groups and do not exhibit optical nonlinearity.

Building blocks $[\text{M}(\text{IO}_3)_6]$ can be condensed into chains (for example in triclinic $\text{Sn}(\text{IO}_3)_4$ (sp.gr. *P*-1) [22]), into layers (in trigonal $\beta\text{-In}(\text{IO}_3)_3$ [2] and $\text{Tl}(\text{IO}_3)_3$ [23] (sp.gr. *R*-3)), and new trigonal $\text{Cs}_3\text{Ta}(\text{IO}_3)_8$ (sp.gr. *P31c*) [24] iodates. For the $\alpha\text{-In}(\text{IO}_3)_3$ [2], $\text{KSc}(\text{IO}_3)_3\text{Cl}$ [18], and for some compounds with divalent M^{II} cations ($\text{LiM}^{\text{II}}(\text{IO}_3)_3$ ($\text{M}^{\text{II}} = \text{Zn}, \text{Cd}$) [25] and $\text{LiMg}(\text{IO}_3)_3$ [26]), a three-dimensional framework of $[\text{M}(\text{IO}_3)_6]$ blocks is described.

Crystal chemical analysis shows that among the iodates, there are modified structural blocks in which the central octahedrons with Ti, V, and Mo atoms have four $(\text{IO}_3)^-$ anionic groups and two O atoms in $\text{LaTiO}(\text{IO}_3)_5$, $\text{Ba}_2\text{VO}_2(\text{IO}_3)_4(\text{IO}_3)$, and $\text{K}_2(\text{MoO}_2(\text{IO}_3)_4$ and $\text{BaMoO}_2(\text{IO}_3)_4 \cdot \text{H}_2\text{O}$, respectively [27]. The same effect was found in the fluorine-containing new iodate $\text{Sn}(\text{IO}_3)_2\text{F}_2$ with a total of four $(\text{IO}_3)^-$ groups and two F atoms [28]. This substitution led to the loss of centrosymmetry and the appearance of polarity and properties in the F-containing iodate.

A new compound $\text{Cs}_5[\text{Sc}_2(\text{IO}_3)_9](\text{IO}_3)_2$ with a framework of $[\text{Sc}(\text{IO}_3)_6]^{3-}$ building blocks was synthesized under mild hydrothermal conditions with a high concentration of iodate component. This work includes characterization of the synthesis of sufficiently large crystals, analysis of the single-crystal structure, and structural relations with other iodates. The unusual pink color of crystals on their surfaces is compared with the case of $\text{BiO}(\text{IO}_3)$ [29]. The correlation of color with growing conditions is discussed.

2. Materials and Methods

Single crystals of a new iodate $\text{Cs}_5[\text{Sc}_2(\text{IO}_3)_9](\text{IO}_3)_2$ were synthesized under mild hydrothermal conditions in highly concentrated solutions. A mixture of standard oxides, analytical grade, and Cs carbonate of $\text{Sc}_2\text{O}_3:\text{Cs}_2\text{CO}_3:\text{I}_2\text{O}_5 = 1:4:8$, which, in mass ratio, corresponded to 0.5 g (3.63 mmol) Sc_2O_3 , 2 g (6.14 mmol) Cs_2CO_3 and 4 g (11.98 mmol) I_2O_5 , was dissolved in 10 mL of distilled water. The solution was hermetically sealed in a 30 mL PTFE-lined stainless steel pressure vessel and stored at $T = 553 \text{ K}$ for 7 days. Final cooling after synthesis to room temperature was carried out within 24 h. The grown crystals were isolated by filtration of the stock solution and washed with hot water.

The experiment revealed two phases. The first was colorless, transparent, and had the shape of predominantly hexagonal flat-prismatic crystals up to 0.5 mm in size. The second phase differed in morphology and was pale pink, transparent, isometric in shape, and up to 2 mm in size. The ratio of mass amounts of both phases was $\sim 1:5$. The overall mass yield of the experiment was close to $\sim 95\%$.

The unit cell parameters for both morphological varieties were determined on single crystals using an XCalibur S diffractometer equipped with a CCD area detector (ω scanning mode) and graphite monochromatic Mo $\text{K}\alpha$ radiation source ($\lambda = 0.71073 \text{ \AA}$). The first phase was known as the trigonal compound $\text{Sc}(\text{IO}_3)_3$, whose symmetry correlated with the morphology of the crystals. The second phase had a monoclinic cell with $a = 21.4044(3)$, $b = 10.86740(14)$, $c = 17.5707(3) \text{ \AA}$, and $\beta = 108.335(2)^\circ$. No such monoclinic unit was found for any compound in ICSD [30], so this phase was proposed as a new one.

Elemental analysis was carried out on crystal surfaces of the new phase using a Jeol JSM-6480LV scanning electronic microscope in combination with WDX analysis. The test revealed the presence of Cs, I, and Sc atoms.

An experimental powder XRD pattern was obtained for morphologically separated crystals of this new iodate phase using an STOE STADY diffractometer ($\text{Cu-K}\alpha$, Figure 1). After crystal structure determination (see below), a theoretical powder pattern (Figure 1) was calculated on the base of the .cif file using the program Powder Cell [31]. The calculated pattern matches well with the experimental one.

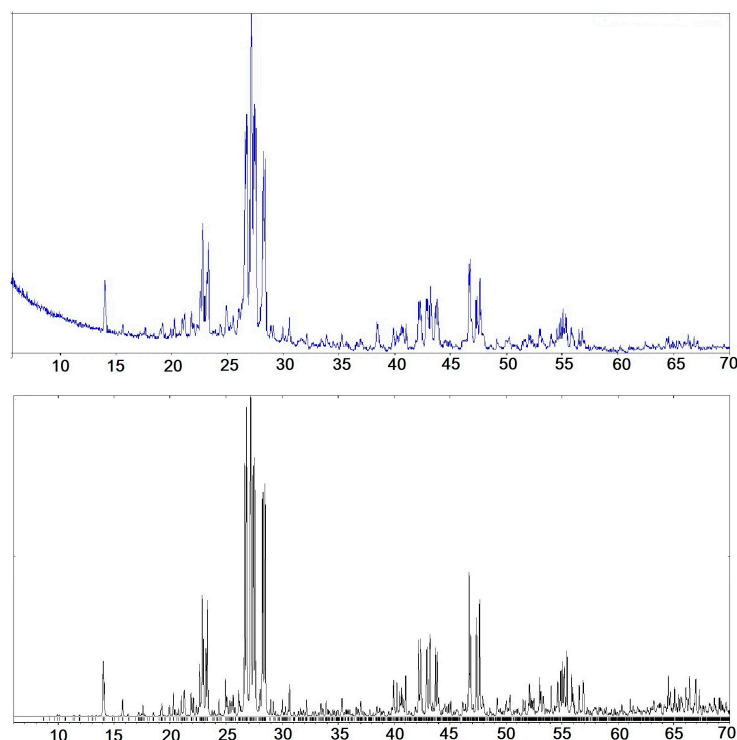


Figure 1. Experimental powder diffraction pattern of $\text{Cs}_5[\text{Sc}_2(\text{IO}_3)_9](\text{IO}_3)_2$ crystals, STOE STADY diffractometer, Cu K α radiation, 2θ -interval 6–70.0°, experimental (**top**), and simulated (**bottom**) powder diffraction pattern.

Second harmonic generation measurements were carried out on the crystalline samples according to the Kurtz and Perry scheme [32] using a Minilite-I YAG:Nd laser operating in Q-switched mode at the repetition rate of 10 Hz at wavelength $\lambda_{\omega} = 1.064$ μm . The incident-beam peak power was about 0.1 MW on a spot 5 mm in diameter on the sample surface. A standard α - SiO_2 powder sample with a 5 μm grain size was used as a reference. The measured signal intensity ($I_{2\omega}$) from the sample was an order less with respect to α -quartz $Q = I_{2\omega}/I_{2\omega}(\text{SiO}_2)$, indicating that crystals of the new phase were centrosymmetric.

An IR spectroscopic study was performed on an “FSM-1201” Fourier spectrometer (Russia) in transmission mode in air at room temperature in the wavenumber range from 400 to 4000 cm^{-1} ; the signal was accumulated over 50 scans at a resolution of 4 cm^{-1} . A sample prepared as a suspension of mineral powder in Vaseline oil was studied. The prepared suspension was applied to a plate of KBr, which was also used as a reference sample before applying the mineral suspension to it.

The spectrum of the studied $\text{Cs}_5[\text{Sc}_2(\text{IO}_3)_9](\text{IO}_3)_2$ sample (Figure 2) is represented by two broad multicomponent absorption bands. According to [33] (p. 179), the high-frequency nine-component band corresponds to the stretching vibrations of the O-I bonds in the “umbrellas” $[\text{IO}_3]^-$. The highest frequency components at 793, 812, and 820 cm^{-1} are symmetrical stretching vibrations (symmetry type A_1 for point symmetry group C_{3v}), and components with absorption maxima at 696, 723, 739, 753, and 767 cm^{-1} belong to the stretching degenerate mode (symmetry type E , C_{3v}). A large number of absorption band components is associated with a decrease in the symmetry of the groups $[\text{IO}_3]^-$ and therefore with a splitting of the E -type vibrations. In addition, factor group splitting of the absorption bands is also possible ($Z = 4$).

A complex absorption band with low intensity and absorption maxima at 420, 432, 450 and 460 cm^{-1} can be attributed to translational vibrations of cation–oxygen. The resulting spectrum does not contain absorption bands related to deformation (angular) vibrations (O-I-O) in the $[\text{IO}_3]$ groups, since the wave numbers of these vibrations are below 400 cm^{-1} .

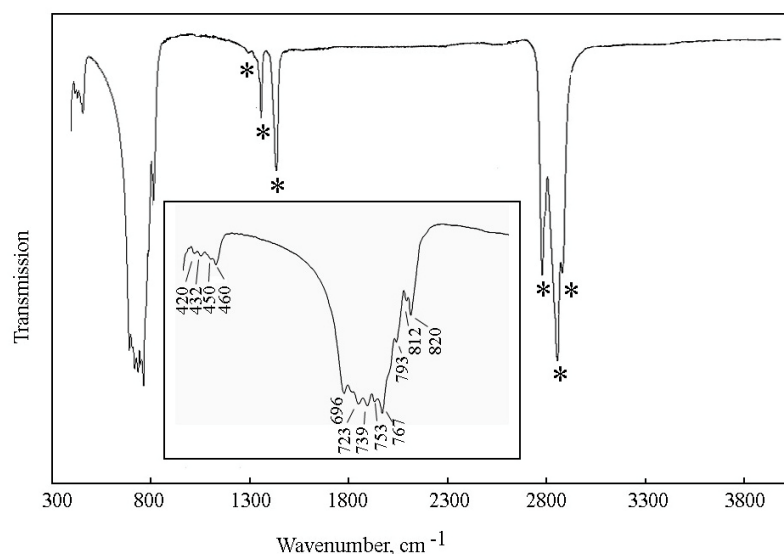


Figure 2. IR absorption spectrum of $\text{Cs}_5[\text{Sc}_2(\text{IO}_3)_9](\text{IO}_3)_2$; *—absorption bands of Vaseline oil.

Differential thermal analyses (DTA) measurements were performed by means of STA 449 F5 Jupiter equipment (Netzsch, Selb, Germany) in the temperature range of 50–1000 °C with a heating rate of 20 °C/min in Ar gas flow. A PtRh20 crucible of 85 μL volume was used in the DTA experiments. The decomposition of the sample (Figure 3) begins at a temperature of 494 °C, with a sharp weight loss and the successive formation of several intermediate phases with decomposition temperatures of 536 and 566 °C. Weight loss in this case is 46%. With further heating, the final stable phase melts at a temperature of 626 °C, the melt decomposes at a rate that increases with increasing temperature up to 914 °C. The weight loss in this case reaches 94% of the initial mass of the sample. The final crystalline phase is stable at 1000 °C and does not experience any phase transitions upon further cooling of the sample to room temperature.

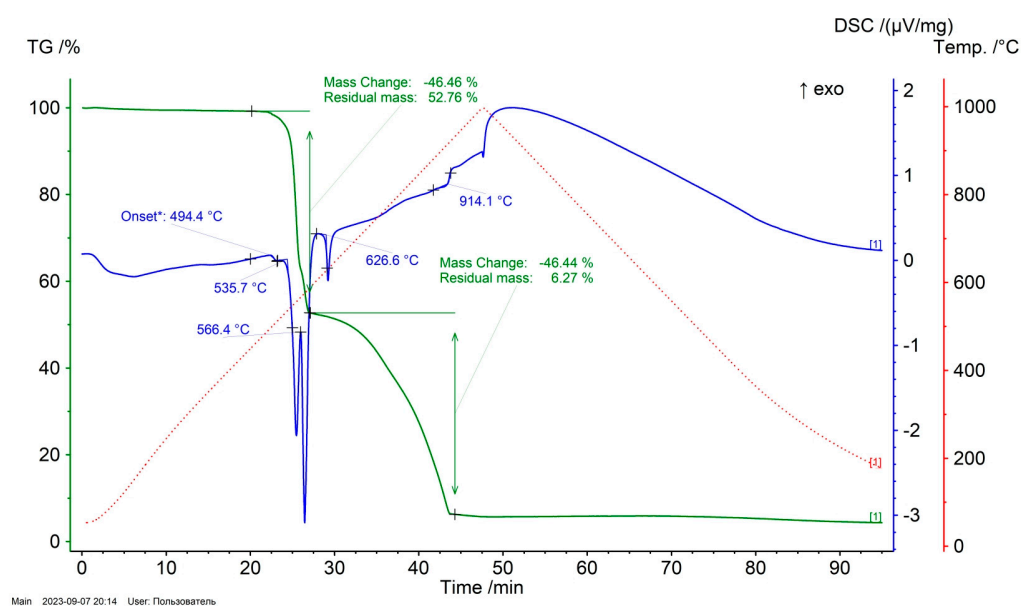


Figure 3. DTA/TG data for new iodate $\text{Cs}_5[\text{Sc}_2(\text{IO}_3)_9](\text{IO}_3)_2$.

3. Results and Discussion

3.1. Single Crystal Structure Determination

For single-crystal X-ray diffraction studies, a transparent isometric crystal with area dimensions of $0.230 \times 0.195 \times 0.140$ mm was selected and glued onto glass fiber (Figure 4).



Figure 4. Image of crystal used in a diffraction experiment from hydrothermal experiments: a colorless transparent crystal has sizes of $0.230 \times 0.195 \times 0.140$ mm.

To collect experimental data, the same diffractometer was used (Table 1) with an exposure time of 20 s per frame and control frames measured during data collection. The data were integrated using the CrysAlis program [34], and the monoclinic $P2_1/c$ space group was proposed. The centrosymmetric space group explains the absence of the SHG signal. The search for a structural model was carried out by direct methods in combination with an analysis of the residual electron density. It was proposed to consider the initial unit cell content to be similar to $K_8Ce_2I_{18}O_{53}$, since this compound had similar cell parameters and volume [35]. The direct method suggested 10 common $4e$ positions of the Cs atom. However, only one was correct, and the remaining nine positions corresponded to I atoms: all I atoms were coordinated by three O atoms from the residual density peaks. I-O distances were standard, and all I atoms had umbrella-like coordination. The number of Cs atoms was large and corresponded to five. In addition, three octahedral-coordinated positions corresponding to Sc atoms were discovered at the residual density: two of them are special ($2a$ and $2b$), with the symmetry of the inversion center. The total amount of oxygen was 33, all in common positions. The final structural result corresponded to the formula $Cs_5[Sc_2(IO_3)_9](IO_3)_2$, $Z = 4$. The structure is confirmed by the Poling valence sum, in which all oxygen atoms are O^{2-} . The experimental data were corrected for absorption in the CrysAlis program [34] using face indexing. The final refinement using SHELXL [36] with the anisotropic approximation of the thermal displacement parameters for all the atoms and the refinement of the weighting scheme led to good structural characteristics. It was proposed to split the O33 position, but this was not taken into account and was explained by a freer temperature displacement of this apical atom in the IO_3 unit. Crystallographic data, atomic coordinates, and selected bonds for the new iodate are presented in Tables 1, S1 and S2, CCDC deposit number 2285771 (see Supplementary Materials). ATOMS and VESTA programs [37,38] were used for the structure visualization.

Table 1. Crystal data and structure refinement of Cs₅[Sc₂(IO₃)₉](IO₃)₂.

Formula	Cs ₅ [Sc ₂ (IO ₃) ₉](IO ₃) ₂
Formula weight, g/mol	2678.37
T, K	293
Crystal system	monoclinic
Space group, Z	<i>P</i> 2 ₁ / <i>c</i> , 4
<i>a</i> , Å	21.4044(3)
<i>b</i> , Å, β, °	10.8674(1), 108.335(2)
<i>c</i> , Å	17.5707(3)
<i>V</i> , Å ³	3879.63(10)
Crystal size, mm	0.230 × 0.195 × 0.140
D _x , g/cm ³	4.586
μ, mm ⁻¹	13.828
F(000)	4656
Wavelength, Å	0.71073
θ range, deg.	2.60–30.82
Limiting indices	−29 ≤ <i>h</i> ≤ 28, −14 ≤ <i>k</i> ≤ 15, −25 ≤ <i>l</i> ≤ 24
Refl. collected/unique	35370/11043 [<i>R</i> _{int} = 0.0481]
Completeness to theta (%)	90.6
Data/restraints/parameters	9560/0/463
GOF (S)	1.145
<i>R</i> ₁ , <i>wR</i> ₂ ¹ [<i>I</i> > 2σ(<i>I</i>)]	0.0396, 0.0842
<i>R</i> ₁ , <i>wR</i> ₂ (all data) ¹	0.0486, 0.0883
Δρ _{max} and Δρ _{min} , e.Å ⁻³	1.654 and −5.170

$$^1 R(F) = \frac{\sum ||F_o| - |F_c||}{\sum |F_o|} \text{ and } wR_2 = \frac{[\sum w(F_o^2 - F_c^2)^2 / \sum w(F_o^2)^2]^{1/2}}{\sum w(F_o^2)^2} \text{ for } F_o^2 > 2\sigma(F_o^2).$$

3.2. Crystal Chemical Features of Cs₅[Sc₂(IO₃)₉](IO₃)₂ and Structural Comparison with Related Iodates, Phosphates, Silicates and Germanates Using Blocks Topology-Symmetry Analysis

The new iodate Cs₅[Sc₂(IO₃)₉](IO₃)₂ has a large unit cell with 52 independent atoms possessing 463 parameters (Table 1 and Table S1); therefore, it is one of the most complex iodate structures, and demonstrates a new structure type. All I1–I11 atoms have typical umbrella-like coordination with regular bonds from 1.773 to 1.842 Å being standard. This coordination can be characterized as pyramidal or tetrahedral, in which the fourth vertex is represented by the I⁵⁺ lone pair. Three independent Sc atoms are coordinated by regular octahedrons located in two special positions at inversion centers and one in a common position. Despite the differences, the octahedra are similar to each other with average Sc–O interatomic distances of 2.079, 2.091, and 2.087 Å (Table S2). The Sc octahedra are surrounded by six IO₃ groups attached via common oxygen vertices. These structural units, or building blocks with the formula [Sc(IO₃)₆]^{3−} (Figure 5a,b), are known in the previously studied iodates mentioned in the introduction. In the new iodate, there is a classical block with six IO₃ groups applied to every oxygen corner; however, the topology and symmetry of the block deviate significantly from the standard trigonal (Figure 5a,b), while the Sc1 and Sc2 blocks are centrosymmetric, and the Sc3 block is asymmetric.

In addition to the IO₃ groups included in the block, there are two positions (I5 and I11) that do not participate in the blocks and are isolated in the structure. The building blocks are connected in chains through common IO₃ umbrellas for each octahedral pair, as in Sn(IO₃)₄ or Sn(IO₃)₂F₂. The chains are slightly curved and consist of triplet [Sc(IO₃)₃]^{3−} blocks. They are extended along the solid diagonal of the monoclinic cell (Figure 5a)—crossing chains run in a diagonal *ac* projection up and down along the *b*-axis. The connection of neighboring chains to the framework occurs through other (IO₃) groups in common pairs of blocks. Thus, of the six (IO₃) groups in the blocks, I6, I1, and I8 connect the Sc octahedra into a framework, and the remaining I2, I9, and I7 belong to the apical IO₃ groups.

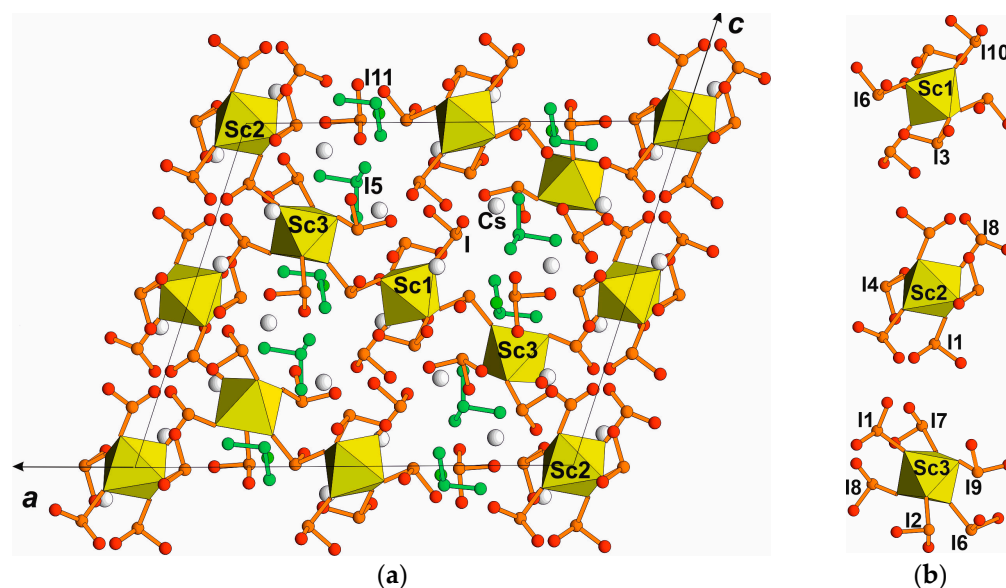


Figure 5. Crystal structure of $Cs_5[Sc_2(IO_3)_9](IO_3)_2$ in ac projection (a); $[Sc(IO_3)_6]^{3-}$ building blocks with centrosymmetric configuration of Sc1 and Sc2 and asymmetric of Sc3 (b); Sc octahedra are shown in yellow, IO₃ groups and Cs atoms are shown as ball-and-stick presentation—Cs in white, I in orange, O in red in IO₃ groups in $[Sc(IO_3)_6]^{3-}$ building blocks, and green for free IO₃ groups.

Five independent Cs atoms demonstrate typical bond lengths with the O atoms up to 3.529 Å and form different polyhedra with coordination numbers (CN) = 8, 9, 6, 7, and 6 for Cs1, Cs2, Cs3, Cs4, and Cs5, respectively. The polyhedral representation shows that the Cs atoms form their own framework (Figure 6), which intercrosses with the previous Sc blocks' framework. A sufficiently large number of Cs atoms significantly determines the topology of the framework—it is the second coordination sphere of the Cs atoms that affects the topology of the blocks and their deviation of trigonal symmetry (Figure 5b).

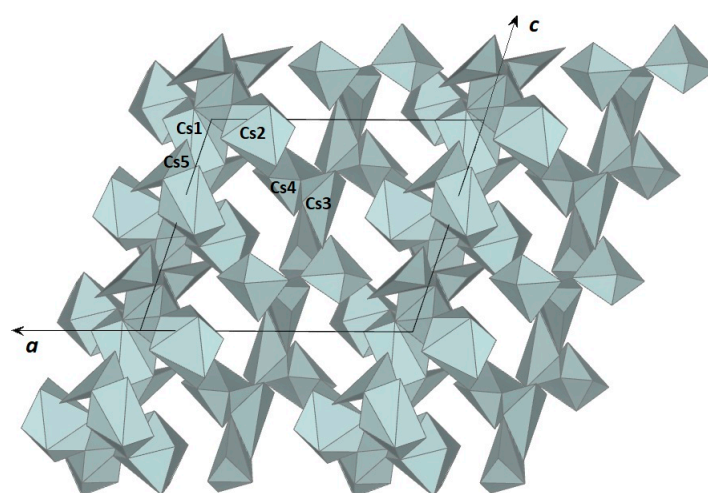


Figure 6. Polyhedral framework composed of Cs polyhedra in the structure $Cs_5[Sc_2(IO_3)_9](IO_3)_2$, ac projection.

The complex iodate $K_8Ce_2I_{18}O_{53}$ [35] with similar cell parameters and volume mentioned before has another type of block $[Ce(IO_3)_8]^{4-}$ with the central Ce^{4+} in a distorted cube and eight (IO₃) groups attached by O vertices. Such blocks are isolated in structure and differ significantly from those described $[Sc(IO_3)_6]^{3-}$.

Among the iodates, $KSc(IO_3)Cl$ [18] is closest to the new $Cs_5[Sc_2(IO_3)_9](IO_3)_2$ structure and has a framework composed of the same building blocks $[Sc(IO_3)_6]^{3-}$. They are

connected by common IO₃ groups; there are no free IO₃ groups in the structure (Figure 7a). It is trigonal, sp.gr. *R*3, and the blocks are more regular because the symmetry of the blocks is higher. K and Cl atoms occupy holes in the framework, alternating levels along the *c*-axis. The smaller ionic radii of K⁺ compared to Cs⁺ resulted in the filling of framework holes without any additional IO₃ groups. The recently studied Cs₃[Ta(IO₃)₆](IO₃)₂ [24] contains iodate layers of [Ta(IO₃)₆][−] blocks, which alternate with isolated IO₃ groups along the *c*-axis (Figure 7b).

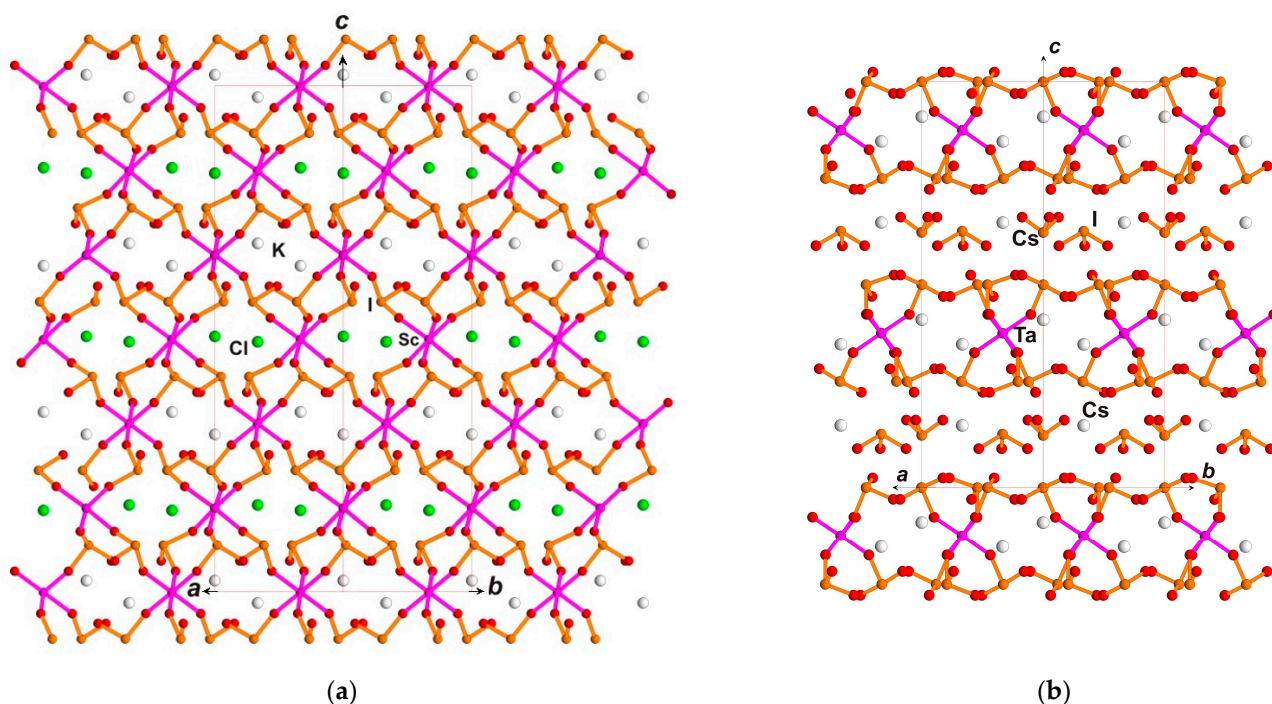


Figure 7. Crystal structures of KSc(IO₃)Cl (a) and Cs₃[Ta(IO₃)₆](IO₃)₂ (b) in diagonal projection. All the atoms are shown in ball-and-stick presentation, K and Cs in white, I in orange, Cl in green, and O in red balls.

The excess of the iodate component during the synthesis was used in the crystallization of both compounds, the new Cs₅[Sc₂(IO₃)₉](IO₃)₂, and the previously studied Cs₃[Ta(IO₃)₆](IO₃)₂. The crystals have an unusual pink color, which was absent for crystal powder, so it belongs to their surface. A similar effect was discovered for BiO(IO₃) crystals treated in special conditions [29], as a result of which the resulting oxygen vacancies on the surface acquired a pink color.

In addition to iodates, similar building blocks with a central M octahedron and six tetrahedra instead of pyramidal IO₃ groups are known for phosphates in the NASICON structure type, silicate minerals such as beryl, benitoite, wadeite, and hilaireite, and synthetic germanates [39]. Some of them are shown in Figure 8a–g. The topology and symmetry of the blocks vary from high symmetrical 32, -3 up to centrosymmetric -1 , or asymmetric 1. The latter is characteristic of building blocks in new iodate compounds (Figure 3b). The positions of IO₃ groups in the blocks are replaced by PO₄, GeO₄, or SiO₄ tetrahedra with a general formula (M(TO₄)₆). The key point is the method of block condensation: for highly charged P⁵⁺ or I⁵⁺, sharing of PO₄ tetrahedra or pyramidal IO₃ groups between octahedral pairs is preferable in contrast to Ge⁴⁺ or Si⁴⁺ tetrahedra with vertex condensation.

One can assume the synthesis of such hypothetical compounds in which both iodate and tetrahedral groups would be present in one block. There is an example of borophosphate with BO₄ and PO₄ tetrahedra in NaIn[BP₂O₈(OH)] [40]. Such blocks would be asymmetric in structure and provide promising properties to the crystals.

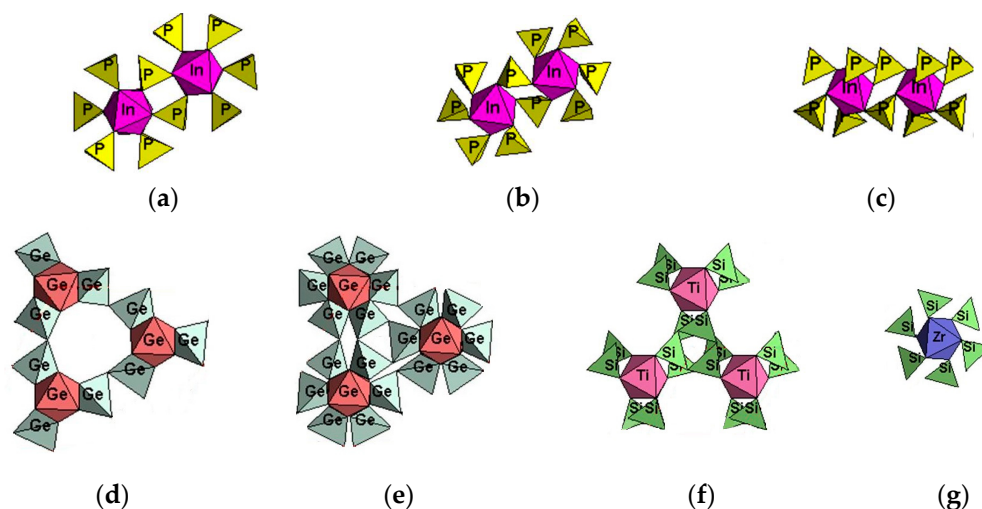


Figure 8. Fundamental building blocks ($M(TO_4)_6$) with M octahedron and six T tetrahedra in phosphates: NASICON-like $Li_{1-x}Ti_{2-x}In_xP_3O_{12}$ (a), $Li_3In_2P_3O_{12}$ (b), $Na_3InP_2O_8$ (c); in germinates: $BaGe_4O_9$ (d), $K_2Ge_4O_9$ (e); in silicates: benitoite $BaTiSi_3O_9$ (f), vadeite $K_2ZrSi_3O_9$ (g).

4. Conclusions

A new iodate $Cs_5[Sc_2(IO_3)_9](IO_3)_2$, sp.gr. $P2_1/c$, $a = 21.4044(3)$, $b = 10.8674(1)$, $c = 17.5707(3)$ Å, $\beta = 108.335(2)^\circ$ was obtained under mild hydrothermal conditions with an excess of the iodate component. It demonstrates a new structure type compared to the previously obtained framework in $KSc(IO_3)_3Cl$ due to additional iodate groups. Another iodate $Cs_3[Ta(IO_3)_6](IO_3)_2$ with a layered structure consisting of blocks and isolated IO_3 groups is maximally enriched in the iodate component. All these related iodates possess similar building blocks ($(M(IO_3)_6)$ ($M = Sc, Ta$)) consisting of an M octahedron and six IO_3 groups connected by O vertices. Such blocks are found in many iodates and present stable structural configurations. Interestingly, the same configuration is valid for phosphates, silicates, and germanates with the replacement of the umbrella-like IO_3 groups (also described as tetrahedral) with six apical PO_4 , SiO_4 , or GeO_4 tetrahedra. The blocks have different topologies and symmetry with point groups of 3, 32, -3 , -1 , and 1 regardless of the class of compounds. They are predominantly isolated from each other, but, in rare structures, are condensed into chains, layers, or frameworks. The method of block condensation is different: highly charged P^{5+} or I^{5+} , tetrahedra, or pyramidal IO_3 groups are shared between octahedral pairs in contrast to vertex condensation of Ge^{4+} or Si^{4+} tetrahedra. The transformation of block symmetry from centrosymmetric to polar due to F introduction or the influence of alkali metals from the second coordination sphere leads to the manifestation of optical nonlinearity, as was discovered in $Sn(IO_3)_2F_2$ [22] or $Rb_3Sc(IO_3)_6$ [17]. The polar orientation of additional isolated IO_3 groups enhances such properties.

Supplementary Materials: The following supporting information can be downloaded at <https://www.mdpi.com/article/10.3390/sym15091777/s1>, Table S1: atomic coordinates and equivalent isotropic displacement parameters (\AA^2) for $Cs_5[Sc_2(IO_3)_9](IO_3)_2$; Table S2: selected interatomic distances for $Cs_5[Sc_2(IO_3)_9](IO_3)_2$.

Author Contributions: Conceptualization and methodology, E.L.B. and O.V.D.; software, O.V.R. and E.L.B.; investigation, O.V.R. and A.S.V.; resources, O.V.D., A.S.V. and E.L.B.; writing—original draft preparation, O.V.R., E.L.B., O.V.D. and A.S.V.; writing—review and editing, E.L.B. and O.V.R.; visualization, O.V.R. All authors have read and agreed to the published version of the manuscript.

Funding: This research received no external funding. The study was performed within the state assignment for Lomonosov Moscow State University “New minerals and synthetic analogues: crystallogenes and crystal chemistry”.

Institutional Review Board Statement: Not applicable.

Informed Consent Statement: Not applicable.

Data Availability Statement: CCDC (ICSD) 2285771 contains crystallographic data for this paper.

Acknowledgments: The authors are grateful to Natalie Zubkova for her aid in the collection of experimental diffraction; to the Laboratory of local methods of materials investigation; to Vasilij Yapaskurt, geological faculty, MSU, for determination of compositions; to Sergey Stefanovich, MSU for SHG measurement; to Victor Maltsev, geological faculty, MSU, for DTA/TG measurements; to Marina Vigasina, geological faculty, MSU, for IR spectroscopy measurements; and to Dmitry Ksenofontov, geological faculty, MSU, for XRPD experimental measurements.

Conflicts of Interest: The authors declare no conflict of interest.

References

1. De Boer, J.L.; van Bolhuis, F.; Olthof-Hazekamp, R.V. Re-investigation of the crystal structure of lithium iodate. *Acta Crystallogr.* **1966**, *21*, 841–843. [[CrossRef](#)]
2. Phanon, D.; Mosset, A.; Gautier-Luneau, I. New materials for infrared nonlinear optic. Syntheses, structural characterisations, second harmonic generation and optical transparency of $M(\text{IO}_3)_3$ metallic iodates. *J. Mater. Chem.* **2007**, *17*, 1123–1130. [[CrossRef](#)]
3. Nguyen, S.D.; Yeon, J.; Kim, S.H.; Halasyamani, P.S. $\text{BiO}(\text{IO}_3)$: A new polar iodate that exhibits an aurivillius-type $(\text{Bi}_2\text{O}_2)^{2+}$ layer and a large SHG response. *J. Am. Chem. Soc.* **2011**, *133*, 12422–12425. [[CrossRef](#)] [[PubMed](#)]
4. Sun, C.-F.; Yang, B.-P.; Mao, J.-G. Structures and properties of functional metal iodates. *Sci. China Chem.* **2011**, *54*, 911–922. [[CrossRef](#)]
5. Hu, C.-L.; Mao, J.-G. Recent advances on second-order NLO/materials based on metal iodates. *Coord. Chem. Rev.* **2015**, *288*, 1–17. [[CrossRef](#)]
6. Mao, F.-F.; Hu, C.-L.; Chen, J.; Wu, B.-L.; Mao, J.-G. $\text{HBa}_{2.5}(\text{IO}_3)_6(\text{I}_2\text{O}_5)$ and $\text{HBa}(\text{IO}_3)(\text{I}_4\text{O}_{11})$: Explorations of second-order nonlinear optical materials in the alkali-earth polyiodate system. *Inorg. Chem.* **2019**, *58*, 3982–3989. [[CrossRef](#)]
7. Abudouwufu, T.; Zhang, M.; Cheng, S.; Zeng, H.; Yang, Z.; Pan, S. $\text{K}_2\text{Na}(\text{IO}_3)_2(\text{I}_3\text{O}_8)$ with Strong Second Harmonic Generation Response Activated by Two Types of Isolated Iodate Anions. *Chem. Mater.* **2020**, *32*, 3608–3614. [[CrossRef](#)]
8. Schellhaas, F.; Hartl, H.T.; Frydrych, R. Die Kristallstruktur von Kaliumhexajodatogermanat(IV). *Acta Crystallogr. Sect. B* **1972**, *28*, 2834–2838. [[CrossRef](#)]
9. Chang, H.-Y.; Kim, S.-H.; Ok, K.M.; Halasyamani, P.S. Polar or Nonpolar? A+ Cation Polarity Control in $\text{A}_2\text{Ti}(\text{IO}_3)_6$ (A = Li, Na, K, Rb, Cs, Tl). *J. Am. Chem. Soc.* **2009**, *131*, 6865–6873. [[CrossRef](#)]
10. Sun, C.-F.; Hu, C.-L.; Kong, F.; Yang, B.-P.; Mao, J.-G. Syntheses and crystal structures of four new silver(I) iodates with d0-transition metal cations. *Dalton Trans.* **2010**, *39*, 1473–1479. [[CrossRef](#)]
11. Kim, Y.H.; Tran, T.T.; Halasyamani, P.S.; Ok, K.M. Macroscopic polarity control with alkali metal cation size and coordination environment in a series of tin iodates. *Inorg. Chem. Front.* **2015**, *2*, 361–368. [[CrossRef](#)]
12. Yang, B.P.; Hu, C.L.; Xu, X.; Mao, J.G. Explorations of New Second-Order Nonlinear Optical Materials in the Potassium Vanadyl Iodate System. *Inorg. Chem.* **2016**, *55*, 2481–2487. [[CrossRef](#)]
13. Liu, H.; Jiang, X.; Wang, X.; Yang, L.; Lin, Z.; Hu, Z.; Meng, X.-G.; Chen, X.; Qin, J. Influence of A-site Cations on Germanium Iodates as Mid-IR Nonlinear Optical Materials: $\text{A}_2\text{Ge}(\text{IO}_3)_6$ (A = Li, K, Rb and Cs) and $\text{BaGe}(\text{IO}_3)_6 \cdot \text{H}_2\text{O}$. *J. Mater. Chem. C* **2018**, *6*, 4698–4705. [[CrossRef](#)]
14. Liu, K.; Han, J.; Huang, J.; Wei, Z.; Yang, Z.; Pan, S. $\text{SrTi}(\text{IO}_3)_6 \cdot 2\text{H}_2\text{O}$ and $\text{SrSn}(\text{IO}_3)_6$: Distinct arrangements of lone pair electrons leading to large birefringences. *RSC Adv.* **2021**, *11*, 10309–10315. [[CrossRef](#)] [[PubMed](#)]
15. Qian, Z.; Wu, H.; Yu, H.; Hu, Z.; Wang, J.; Wu, Y. New Polymorphism for $\text{BaTi}(\text{IO}_3)_6$ with Two Polymorphs Crystallizing in the Same Space Group. *Dalton Trans.* **2020**, *49*, 8443–8447. [[CrossRef](#)] [[PubMed](#)]
16. Xiao, L.; You, F.; Gong, P.; Hu, Z.; Lin, Z. Title Synthesis and Structure of a new Mixed Metal Iodate $\text{Ba}_3\text{Ga}_2(\text{IO}_3)_{12}$. *CrystEngComm* **2019**, *21*, 4981–4986. [[CrossRef](#)]
17. Reutova, O.; Belokoneva, E.; Volkov, A.; Dimitrova, O.; Stefanovich, S. Two New $\text{Rb}_3\text{Sc}(\text{IO}_3)_6$ Polytypes in Proposed Nonlinear Optical Family $\text{A}_3\text{M}(\text{IO}_3)_6$ (A = K, Rb; M = Sc, In): Topology–Symmetry Analysis, Order–Disorder and Structure–Properties Relation. *Symmetry* **2022**, *14*, 1699. [[CrossRef](#)]
18. Vagourdi, E.M.; Zhang, W.; Denisova, K.; Lemmens, P.; Halasyamani, P.S.; Johnsson, M. Synthesis and Characterization of Two New Second Harmonic Generation Active Iodates: $\text{K}_3\text{Sc}(\text{IO}_3)_6$ and $\text{KSc}(\text{IO}_3)_3\text{Cl}$. *ACS Omega* **2020**, *5*, 5235–5240. [[CrossRef](#)]
19. Liu, X.; Li, G.; Hu, Y.; Yang, M.; Kong, X.; Shi, Z.; Feng, S. Hydrothermal Synthesis and Crystal Structure of Polar and Nonpolar Compounds in Indium Iodate Family. *Cryst. Growth Des.* **2008**, *8*, 2453–2457. [[CrossRef](#)]
20. Yang, B.-P.; Sun, C.-F.; Hu, C.-L.; Mao, J.-G. A series of new alkali metal indium iodates with isolated or extended anions. *Dalton Trans.* **2011**, *40*, 1055–1060. [[CrossRef](#)]
21. Reutova, O.V.; Belokoneva, E.L.; Dimitrova, O.V.; Volkov, A.S. Synthesis and Crystal Structure of New Iodate $\text{Na}_3\text{Fe}[\text{IO}_3]_6$ of the $\text{A}_3\text{M}[\text{IO}_3]_6$ Structural Family (A = Na, K, Rb, Cs, Tl; M = Ti, Fe, Ge, In, Pt). *Crystallogr. Rep.* **2020**, *65*, 428–432. [[CrossRef](#)]
22. Luo, M.; Liang, F.; Hao, X.; Lin, D.; Li, B.; Lin, Z.; Ye, N. Rational Design of the Nonlinear Optical Response in a Tin Iodate Fluoride $\text{Sn}(\text{IO}_3)_2\text{F}_2$. *Chem. Mater.* **2020**, *32*, 2615–2620. [[CrossRef](#)]

23. Yeon, J.; Kim, S.-H.; Halasyamani, P.S. New thallium iodates—Synthesis, characterization, and calculations of $\text{Tl}(\text{IO}_3)_3$ and $\text{Tl}_4(\text{IO}_3)_6$, $[\text{Tl}+3\text{Tl}_3+(\text{IO}_3)_6]$. *J. Solid State Chem.* **2009**, *182*, 3269–3274. [[CrossRef](#)]
24. Belokoneva, E.L.; Reutova, O.V.; Dimitrova, O.V.; Volkov, A.S.; Stefanovich, S.Y.; Maltsev, V.V.; Viganina, M.F. New layered nonlinear optical iodate $\text{Cs}_3\text{Ta}(\text{IO}_3)_8$: Topology-symmetry analysis and structure prediction. *CrystEngComm* **2023**, *25*, 4364–4369. [[CrossRef](#)]
25. Jia, Y.-J.; Chen, Y.-G.; Guo, Y.; Guan, X.-F.; Li, C.; Li, B.; Liu, M.-M.; Zhang, X.-M. $\text{LiMII}(\text{IO}_3)_3$ (MII = Zn and Cd): Two Promising Nonlinear Optical Crystals Derived from a Tunable Structure Model of $\alpha\text{-LiIO}_3$. *Angew. Chem. Int. Ed.* **2019**, *58*, 17194–17198. [[CrossRef](#)] [[PubMed](#)]
26. Chen, J.; Hu, C.-L.; Mao, F.F.; Zhang, X.-H.; Yang, B.-P.; Mao, J.-G. $\text{LiMg}(\text{IO}_3)_3$: An excellent SHG material designed by single-site aliovalent substitution. *Chem. Sci.* **2019**, *10*, 10870–10875. [[CrossRef](#)] [[PubMed](#)]
27. Ok, K.M.; Halasyamani, P.S. New d^0 transition metal iodates: Synthesis, structure, and characterization of $\text{BaTi}(\text{IO}_3)_6$, $\text{LaTiO}(\text{IO}_3)_5$, $\text{Ba}_2\text{VO}_2(\text{IO}_3)_4(\text{IO}_3)$ and $\text{K}_2\text{MoO}_2(\text{IO}_3)_4$ and $\text{BaMoO}_2(\text{IO}_3)_4 \cdot \text{H}_2\text{O}$. *Inorg. Chem.* **2005**, *44*, 2261–2271. [[CrossRef](#)] [[PubMed](#)]
28. Luo, M.; Liang, F.; Yao, X.; Lin, D.; Li, B.; Lin, Z.; Ye, N. Rational chemically tailoring design of the tin iodate fluoride $\text{Sn}(\text{IO}_3)_2\text{F}_2$ as a potential nonlinear optical material. *Chem. Mat.* **2020**, *32*, 2615–2620. [[CrossRef](#)]
29. Ling, Y.; Li, J.; Wu, J.; Liu, H.; Mao, X.; Qi, Y.; Ma, Q.; Liu, Q.; Qiao, Z.; Chu, W. Enhanced photocatalytic activity on elemental mercury over pink BiOIO_3 nanosheets with abundant oxygen vacancies. *Korean J. Chem. Eng.* **2022**, *39*, 343–352. [[CrossRef](#)]
30. The Cambridge Crystallographic Data Centre (CCDC). Inorganic Crystal Structure Data Base—ICSD. Available online: <https://www.ccdc.cam.ac.uk/> (accessed on 31 July 2020).
31. Kraus, W.; Nolze, G. POWDER CELL—A program for the representation and manipulation of crystal structures and calculation of the resulting X-ray powder patterns. *J. Appl. Cryst.* **1996**, *29*, 301–303. [[CrossRef](#)]
32. Kurtz, S.K.; Perry, T.T. A Powder Technique for the Evaluation of Nonlinear Optical Materials. *J. Appl. Phys.* **1968**, *39*, 3798–3813. [[CrossRef](#)]
33. Nakamoto, K. *Infrared and Raman Spectra of Inorganic and Coordination Compounds*, 6th ed.; John Wiley and Sons, Inc.: Hoboken, NJ, USA, 2009; 427p.
34. Agilent Technologies. *CrysAlisPro Software System*, version 1.171.3735; Agilent Technologies UK Ltd.: Oxford, UK, 2014.
35. Wu, R.; Jiang, X.; Xia, M.; Liu, L.; Wang, X.; Lin, Z.; Chen, C. $\text{K}_8\text{Ce}_2\text{I}_{18}\text{O}_{53}$: A novel potassium cerium(IV) iodate with enhanced visible light driven photocatalytic activity resulting from polar zero dimensional $[\text{Ce}(\text{IO}_3)_8]_4$ —units. *Dalton Trans.* **2017**, *46*, 4170–4173. [[CrossRef](#)] [[PubMed](#)]
36. Sheldrick, G.M. *SHELXL-97, a Program for Crystal Structure Refinement; SHELXS-97, a Program for Automatic Solution of Crystal Structures*; University of Goettingen: Goettingen, Germany, 1997.
37. Dowty, E. *Atoms 3.2—A Computer Program for Displaying Atomic Structures*; Kingpost: Kingpost, TN, USA, 1995.
38. Momma, K.; Izumi, F. VESTA 3 for three-dimensional visualization of crystal, volumetric and morphology data. *J. Appl. Crystallogr.* **2011**, *44*, 1272–1276. [[CrossRef](#)]
39. Gurbanova, O.A.; Belokoneva, E.L. Topology-symmetry analysis of the mixed frameworks in the structures of phosphates, germanates, gallates, and silicates based on fundamental building blocks. *CrystReports* **2006**, *51*, 577–583. [[CrossRef](#)]
40. Gurbanova, O.A.; Belokoneva, E.L.; Dimitrova, O.V. Synthesis and crystal structure of the new borophosphate $\text{NaIn}[\text{BP}_2\text{O}_8(\text{OH})]$. *Russ. J. Inorg. Chem.* **2002**, *47*, 10–13.

Disclaimer/Publisher’s Note: The statements, opinions and data contained in all publications are solely those of the individual author(s) and contributor(s) and not of MDPI and/or the editor(s). MDPI and/or the editor(s) disclaim responsibility for any injury to people or property resulting from any ideas, methods, instructions or products referred to in the content.